Probing the compressive failure mechanism in syntactic foam using X-ray micro-computed tomography

Mehmet E. Kartal[1,2]

[1]Lloyd's Register Foundation Centre for Safety & Reliability Engineering, School of Engineering, University of Aberdeen, Aberdeen AB24 3UE, UK

[2]School of Engineering, University of Aberdeen, Aberdeen, AB24 3UE, UK

Corresponding author. Tel.: +44 1224 272495 E-mail: mehmet.kartal@abdn.ac.uk

Abstract This study aims at characterising the compressive damage mechanisms occurring in syntactic foam containing micro-glass spheres. For this purpose, X-ray micro-computed tomography integrated with an in-situ compressive testing stage was employed for acquiring three-dimensional images at different stages of compressive strains. It has been found that damage is initiated at the weakest micro-spheres. When uniaxial applied strain is increased, shear collapse bands (SCB) develop around the fragmented micro-spheres due to stress concentration. SCBs are thickened with increase in compressive loading.

Introduction

Syntactic foams are low-density materials fabricated by randomly filling hollow particles into a material matrix. Hollow particles have a significant effect on the properties of syntactic foams. Their microstructure is determined by the choice of particle materials, volume fraction and wall thickness of particles. Commonly used hollow particles in polymer matrix syntactic foams are glass, ceramic and fly ash cenospheres [1].

Hollow glass is one of the most commonly used particles, as they confer a variety of valuable properties such as low density, impact strength, thermal insulation, dimensional stability and low dielectric constant. In recent years, they are becoming more widely used as thermal installation in the offshore oil extraction industry [1-4], being utilised in the subsea flowlines used to bring the oil from the extraction point up to the surface. The syntactic foams are subjected to high pressure especially in deep water and must be durable in such harsh conditions as the deep sea environment. Therefore, a better understanding of the in-service failure mechanisms represent an important engineering challenge as a service-life of at least a couple of decades is envisaged.

Since syntactic foams possess complex and heterogeneous microstructures their evaluations should be made in three dimensions. Although, scanning electron microscopy (SEM) provides very high resolution imaging, results are only limited to the free surface of a specimen. Recently, X-ray computed tomography has become an attractive characterisation technique in Materials Science as multiscale material behaviours can be obtained without sectioning specimens. With the very rapid growth of instrumentation over the last 15 years, it is now possible to obtain 3D images with a spatial resolution less than a micrometer by means of lab-based X-ray computed tomography.

Experimental procedure

The material used in this investigation was syntactic foam provided by Trelleborg. The epoxy matrix was made through a batch mixing process with a post cure (anhydride catalyst). The glass spheres used adhered to the company's (3M) K25 specifications, given in Table 1. Prismatic blocks were machined from a bar with the dimensions $10 \times 10 \times 10$ mm^3.

Table 1: Glass sphere properties provided by the manufacturer 3M

Particle Size (µm, volume) Distribution			Effective top size(µm)	True Density (g/cc)	Target Crush Strength (90% survival, psi)
10th%	50th%	90th%			
25	55	90	105	0.25	750

X-ray micro-computed tomography was conducted using the lab based ZEISS VersaXRM-410 machine, which has a minimum spatial resolution of 0.9 µm, minimum voxel size of 0.1 µm, a maximum power output and voltage of 10 W and 150 kV respectively. A micro tension/compression testing stage with a ±5kN capacity load cell (Deben, UK) was mounted on the stage of the X-ray machine. Figure 1 shows the experimental configuration indicating key features such as the X-ray source, detector and tension/compression testing rig. The sample was loaded into the Deben rig at a central position in a 3mm thick vitreous glassy carbon tube providing low X-Ray attenuation. The specimen was scanned at 13 different deformation stages and nominal strains of 37% were reached in compressive tests.

The pixel size was 1.7µm for 1024×1024 pixel projection images. Sets of 2400 were captured over 360° of sample rotation. The 2D radiographs were reconstructed into 3D images. Post processing analysis of the data obtained was possible using Avizo computer software.
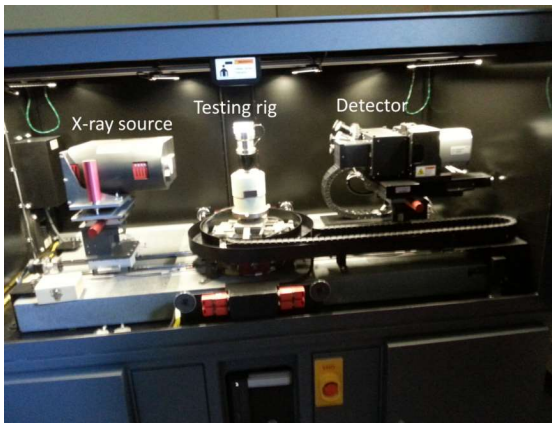
Fig.1: Photograph of apparatus in-situ, showing X-ray source, detector and tension/compression rig
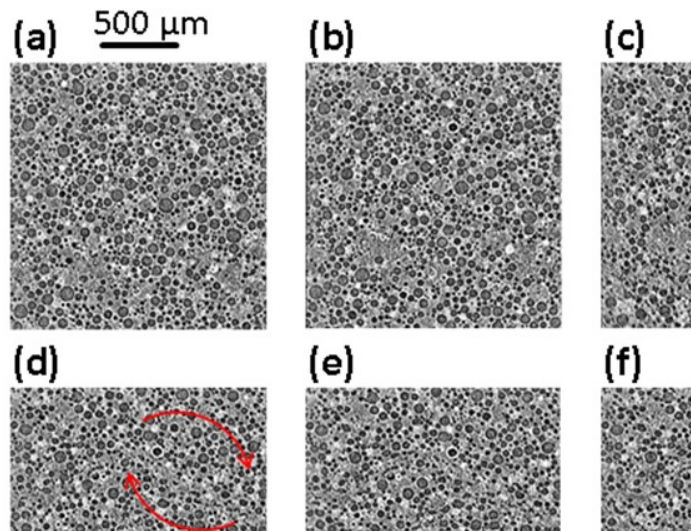
Fig.2 Internal microstructure and failure process of the syntactic foam obtained from µ-CT at different strains a) 0.0, (b) −4.2%, (c) −5.8%, (d) −8.6%, (e)−11.1%, (f) −13.7%

Results and Discussion

We observed the microstructures and damage accumulation under 13 different engineering compressive strains. In order to fit the images on the paper, 6 of them will be presented here obtained under the strain values of 0.0%, −4.2%, −5.8%, −8.6%, −11.1% and −13.7%.

Fig.2 shows the XZ planes of the 3D images produced from the X-ray computed tomography at 6 different levels of strain. All of the images are given to the same scale (1.74mm by 1.74mm), with the load being applied in the vertical upward direction.

Fig. 2a shows the natural state of the syntactic foam under the very light load (i.e. −10 N). In Fig 2b, deformation is elastic and the syntactic foam is observed to move in the vertical upward direction without observing any damage or failure of microspheres. The subsequent image was taken shortly after the specimen was observed to reach its compressive strength during the compression test (Fig. 2c). Here, damage has already initiated with several microspheres already fragmented especially at the bottom of the region of interest. In addition, a shear collapse band (SCB) developed local to the fragmented microspheres due to stress concentration as highlighted in Fig. 2c. As expected from syntactic foams with high volume fraction of microspheres, slip bands evolve diagonally. When the compressive strain reached the value of −8.6% in Fig. 2d, the movement of the particles in the vertical direction is not observed but a bending deformation mechanism around the SCB band is observed.

In Fig. 2e, there are two more thickened SCBs developed and they met each other as shown with the light lines. In Fig. 2f, as the two shear bands interacted each other, the direction of the SCB at the bottom of the right hand side of the image changed and almost combined with the other SCB at the bottom of the left hand side of the image. During this damage process, crushed microspheres were piled up in this region. Note that greater explanation can be found in the author's previous publication [5].

The comparison of the microstructural changes of the syntactic foam obtained from different sets of experiments (also see reference [5]) during compressive tests show that SCBs develop at different random locations in the specimen. This can be explained by the phenomenon that relatively weak spheres are first crushed and then induce the damage of surrounding microspheres to form SCBs due to minimal energy-consumption. The quasi-static initial failure stress depends on the strength of the weakest microspheres.

Conclusion

In-situ compression testing was carried out with X-ray micro-computed tomography allowing full-field, high-resolution 3D observation of deformation. The results suggest that failure initiates at weak microspheres and propagates from these locations. A number of concurrent failure mechanisms occur including: crushing of individual microspheres, formation of shear collapse bands (SCBs) diagonal to the loading direction, accompanying bending deformation and subsequent thickening of the SCBs as regions of fragmented microspheres expand.

References

[1]   D. Pinisetty, V.C. Shunmugasamy and N. Gupta (2015). Hollow Glass Microspheres for Plastics, Elastomers, and Adhesives Compounds, pp. 147-174, edited by, S.E. Amos and B. Yalcin, Elsevier.
[2]   L Bardella and F Genna (2001). International Journal of Solids and Structures, vol. 38 (40-41), pp. 7235–7260.
[3]   J. Adrien, E. Maire, N. Gimenez and V. Sauvant-Moynot (2007). Acta Materialia, vol., 55, pp., 1667–1679.
[4]   N. Gupta, S. E. Zeltmann, V. C. Shunmugasamy and D. Pinisetty (2013). The Journal of the Minerals, Metals & Materials Society, vol. 66(2), pp. 245–254.
[5]   M.E. Kartal, L.H.Dugdale., J.J. Harrigan, M.A. Siddiq, D. Pokrajac,, D.M. Mulvihill (2017). Journal of Materials Science, vol. 52(17), pp. 10186-10197.